MATHEMATICAL BIOSCIENCES
AND ENGINEERING
Volume **2**, Number **1**, January **2005**

http://www.mbejournal.org/

pp. **53–77**

FROM NET TOPOLOGY TO SYNCHRONIZATION IN HR NEURON GRIDS

Stefano Cosenza,[1] Paolo Crucitti,[1,2] Luigi Fortuna,[1]
Mattia Frasca,[1] Manuela La Rosa,[1,3]
Cecilia Stagni,[1] and Lisa Usai[1]

[1] DIEES, University of Catania, Viale Andrea Doria 6, 95123, Catania
[2] Scuola Superiore di Catania, Via S. Paolo 73, 95123, Catania
[3] SST group, Corporate R&D, ST Microelectronics, Stradale Primosole 50, 95100, Catania

(Communicated by Stefano Boccaletti)

Abstract. In this paper, we investigate the role of topology on synchronization, a fundamental feature of many technological and biological fields. We study it in Hindmarsh-Rose neural networks, with electrical and chemical synapses, where neurons are placed on a bi-dimensional lattice, folded on a torus, and the synapses are set according to several topologies. In addition to the standard topologies used in other studies, we introduce a new model that generalizes the Barabási-Albert scale-free model, taking into account the physical distance between nodes. Such a model, because of its plausibility both in the static characteristics and in the dynamical evolution, is a good representation for those real networks (such as a network of neurons) whose edges are not costless. We investigate synchronization in several topologies; the results strongly depend on the adopted synapse model.

1. **Introduction.** Many real systems can be modelled as complex networks. Several examples can be found: at a social level, the simplest network is the organization of people; nations can organize themselves at a political and economic level, where global economy is a network of national economies, in turn composed of networks of markets, which are themselves networks of producers and consumers; networks of routers (as the Internet); networks of Web pages (as the World Wide Web); networks of the diffusion of energy in living organisms, in infrastructures created by humans, or in many physical systems; and networks of neurons (as the brain) [1]. It is important not only to understand how networks arise and develop but also to investigate their properties and their dynamical behavior. As for dynamical behavior, synchronization, being a common feature of many dynamical systems [1], has been studied in many applications, such as coupled damped and forced pendulums [2] or arrays of Chua's circuits [3]. Recent studies have devoted particular attention to the development of two main branches: the first analyzing how spatial diversity can give rise to significant improvements in the synchronization process [4, 5, 6, 7, 8, 9] and the second considering the effect of the topology of the network of coupled systems on the dynamical behavior [10, 11, 12, 13]. It has been shown, in fact, that a systems's structure affects its function [14] and

2000 *Mathematics Subject Classification.* 92C29.
Key words and phrases. Hindmarsh-Rose neuron, synchronization, electrical and chemical synapse, regular lattice, small-world network, scale-free network, random graph.

influences the way in which information is exchanged; for instance, it influences the spread of disease and, in Internet, the tendency for routers to move towards synchrony [15].

The research concerning synchronization has been inspired mostly by biology [16, 17], from the flashing of fireflies to the chirps of crickets, from the wave propagation in the heart to information processing of neurons. In particular, the study of the dynamics of a neural network is a central topic for many sciences, since the primary aim is a complete and satisfactory representation of the physiology of the neuron system, even to design artificial biologically inspired systems. Synchronization of neural networks is important because it underlies several behaviors, such as learning and generation of rhythmic movements for motor control.

However, we are so far from having an in-depth knowledge of either the mechanisms of the neuronal activity or the real structure of a neural network that researchers must restrict their analysis either to very accurate topologies or to very accurate neuron models [18].

In this paper, we choose a compromise solution that considers an intermediate level of accuracy both for topological and neural models: we investigate the role of topology on a bi-dimensional surface of Hindmarsh-Rose neurons coupled by means of electrical or chemical synapses.

The analyzed topologies belong to two different classes: static (where the number of nodes and edges is constant in time) and dynamical (where at each time step a new node and some edges are added).

Different neural networks, characterized by different topologies and different synapses, have been compared and characterized by means of both static parameters, which take into account only the structure, and dynamic parameters, which take into account the temporal evolution of the state variables of neurons.

Among the parameters shown to analyze the networks, we have also included a cost parameter with a two-fold aim: on one side it allows one to take into account the role that physical distance plays in the formation of new synapses (edges) between neurons (nodes); on the other it can be a fundamental parameter for the design of artificial neuron networks.

In section 2, we present a quick review of recent developments in network modelling, and we define a new generalization of the Barabási-Albert model, based on the plausible hypothesis that physical distance between nodes in a network is a fundamental parameter in the process of links formation. In section 3, we describe the Hindmarsh-Rose neuron and the models we used to represent the electrical and chemical synapses. In section 4, we introduce the parameters we used to evaluate synchronization and energetic costs. In section 5, we present some results with electrical and chemical synapses, comparing the topologies that we use according to the previously applied parameters. Finally, in section 6, we draw a conclusion.

2. **Topological models.** A generic network is a graph G, in which the N nodes represent the basic component of the network and the K edges represent an interaction between them: for example, in the Internet [19], nodes are routers and edges are physical connections between them; in a neural network [10], nodes are neurons and edges are synaptic connections between them. We represent a network through its adjacency matrix $A = (a_{ij})$, whose element a_{ij} is 1 if there is an edge connecting nodes i and j, and 0 otherwise. The network is undirected and has an average degree (number of first neighbors of each node) equal to $< k >= 2 \cdot K/N$.

To characterize the topological properties of networks, we use two parameters, as defined in [20]. The first is the *characteristic path length L*:

$$L(\mathbf{G}) = \frac{\sum_{i \neq j \in \mathbf{G}} d_{ij}}{N(N-1)}, \tag{1}$$

where d_{ij} is the length of the shortest path connecting nodes i and j. A small value of L indicates good global properties of the network.

The second parameter is the *clustering coefficient C*, defined as:

$$C(\mathbf{G}) = \frac{\sum_{i \in \mathbf{G}} C_i}{N}, \tag{2}$$

with

$$C_i = \frac{number\ of\ egdes\ in\ G_i}{k_i \cdot (k_i - 1)/2}, \tag{3}$$

where $k_i \cdot (k_i - 1)/2$ is the total number of possible edges in G_i, which is the subgraph of the first neighbors of the node i. A large value of C is an index of good local properties, because it indicates that there are many connections between nodes belonging to the same neighborhood.

These structural properties do not take into account that in real networks connections between nodes may have a cost related to the physical distance between the nodes [21]. To evaluate how much the building cost of a network is, we introduce a new parameter. This is the *structural cost* of the network as the total physical length of the edges present in the system defined as follows:

$$Cost(\mathbf{G}) = \sum_{i,j \in \mathbf{G}} a_{ij} \cdot l_{ij}, \tag{4}$$

where a_{ij} is the element ij of the adjacency matrix and l_{ij} is the Euclidean distance between nodes i and j.

2.1. **Brief summary of topological models.** In this section, we summarize the main properties of the topological models investigated in this paper. We consider nodes placed on a bi-dimensional surface with periodic boundary conditions so that the surface is a torus and edge effects are avoided.

The first topology is the well-known regular lattice. Nodes are placed in a regular way, forming a grid, and each of them has the same number of edges; that is the same degree. Because the connections are only local, communication between two distant nodes can occur only by means of many other intermediate nodes. Hence, the *characteristic path length L* for the lattice is high. Local connections, on the contrary, make the network clustered, leading to high values of C.

The Erdös-Rényi (ER) random graph [22] is the most investigated graph in the literature. It starts from an initial condition of N nodes and no edges and then K edges are added between couples of randomly selected nodes. Because nodes are chosen at random, they will not have the same number of edges, as in the case of a lattice, and the degree will have a Poissonian distribution. The ER model has good global properties. In fact, the *characteristic path length*, increasing slowly with N, is quite small even in a fairly large network. On the other hand, it has poor local properties, having a low *clustering coefficient*.

Lattice and ER graph are based on two opposite concepts: the former on regularity and the latter on randomness. However, real-world networks are neither completely regular nor completely random [20], but stay in between. Starting

from this consideration, Watts and Strogatz developed the small-world model. The Watts-Strogatz model (WS) starts from an initial condition of a regular graph (a regular lattice, in our case), and one edge at a time is considered: with probability p, it is cut at an extremity and reconnected to a randomly selected node (rewiring). The model thus ranges from the regular lattice ($p = 0$) to the random graph ($p = 1$). Watts and Strogatz showed that it is sufficient to rewire a small number of edges (i.e., a small value of the probability p sufficies) in order to have small L and large C, i.e. both good global and local properties.

One of the main drawbacks of the WS model is that because of the rewiring process, the network can become non-connected. To avoid this situation, Newman and Watts [23] have developed a new model in which edges are simply added with probability q. The Newman-Watts (NW) model ranges from the regular lattice ($q = 0$) to the fully connected network ($q = 1$).

All the networks presented above show a high homogeneity in the node degree. Nevertheless, many real-world networks [19, 24] are not so democratic, showing a power-law $P(k) \sim k^{-\gamma}$ with an exponent γ that usually ranges between 2 and 3.

To meet the requirement of plausibility in the degree distribution, Barabási and Albert [25] have developed a model that, starting from an initial condition of a network of few nodes [26], dynamically evolves according to *growing* (at each time step a new node is inserted into the network) and *preferential attachment*: the new node is connected to m already existing nodes [27] with a probability proportional to the degree of those nodes. The probability that the new node i is connected to the node j is given by the following relation:

$$\Pi(j) = \frac{k_j}{\sum_{h \in \mathbf{G}} k_h}, \tag{5}$$

where k_h is the degree of node h.

2.2. **Generalized Barabási-Albert (GBA) scale-free model.** Although the Barabási-Albert (BA) model is a good representation for a huge variety of real-world networks, it cannot reproduce the characteristics of those systems in which edges are not costless (e.g., power grids or neural networks). To overcome this problem, we introduce a new generalization of the BA model for networks with a precise spatial arrangement. Initial condition and growing process are the same of the BA model, previously described. The only difference in comparison with the original BA model is that now in the preferential attachment we take into consideration the physical distance between nodes, stating that the probability for an edge to be constructed is inversely proportional to a power of the distance. The probability for a new node i to be connected with an already present node j is

$$\Pi(j) = \frac{k_j}{l_{ij}^b} \cdot \frac{1}{\sum_{h \in \mathbf{G}} \frac{k_h}{l_{ih}^b}}, \tag{6}$$

where k_h is the degree of node h, l_{ih} is the Euclidean distance between nodes i and h, and b is an exponent that weights the distance in comparison with the degree. The greater the exponent b is the greater the importance of distance (in comparison with the degree) in the model evolution. Of course, a value of $b = 0$ leads to the original BA model. An example of a GBA network with $N = 196$ nodes and $< k >= 4$ is shown in Figure 1.

Because the network topology is introduced here for the first time, we briefly provide a further characterization of the network. The properties of a network

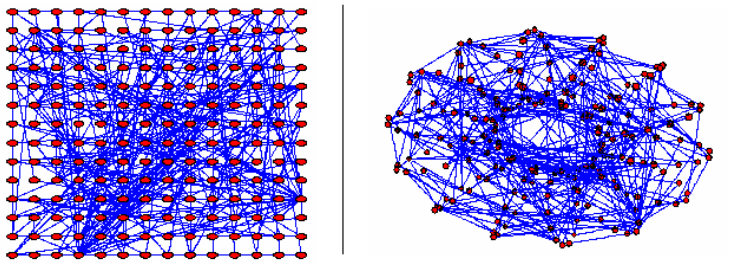

FIGURE 1. Generalized Barabási-Albert scale-free model with $N = 196$ nodes, average degree $< k >= 4$ and exponent b=3. We show the bi-dimensional view on the left and the three-dimensional view on the right.

with a larger number of nodes have been investigated. In Figure 2, the cumulative degree distribution $P(k)$ is plotted in a log-log scale for nine different values of the exponent b, for networks with $N = 10,000$ nodes and average degree $< k >= 8$. For small values of this parameter b (up to $b = 3$), the degree distribution preserves the power-law decay typical of the BA model. However for values of b larger than 3, the degree distribution is no longer scale-free, and the network tends toward homogeneity: in the original BA model ($b = 0$), the most connected node has a huge number of links (almost 400), while with an exponent $b = 4$, the highest degree in the network is reduced to about 90.

Though the exponent γ of the power-law varies with the number of nodes present in the network, it seems to saturate for large networks. For low values of the parameter b (up to $b = 3$) –that is i.e. for those values for which the power law is better preserved– we have not found wide variations of the exponent γ, which ranges between 2.5 and 3.0.

To characterize the model introduced here, we have calculated the *characteristic path length* L, the *clustering coefficient* C, and the *structural cost*, as functions of the exponent b for networks with $N = 10,000$ nodes and average degree $< k >= 8$ (see Fig. 3).

The results show that the *characteristic path length* is almost unaffected by increasing b, if compared to the range of variation from the totally connected network (for which $L \approx 0.03 \cdot L(Lattice)$) to the regular lattice. On the contrary, the increasing weight of the distance in the preferential attachment, causes a significant improvement of the *clustering coefficient* that, starting from the 0.03% for $b = 0$, saturates for $b \approx 8$ at about 98% of the corresponding value for a regular lattice. Moreover, as far as we increase the exponent b, long-range connections are hampered and, consequently, the cost decreases: moving from $b = 0$ to $b = 4$, it is reduced from about thirty-two times to about two times the cost of the lattice.

In Figure 4, we show how the *characteristic path length* L scales with the size N of the network, for the GBA model with an exponent $b = 3$. The results are typical of the small-world effect: L grows with the logarithm of the size ($L \sim \ln N$).

Therefore there is a region, with b nearly equal to 3, for which we have a network with scale-free degree distribution, low *characteristic path length* that scales with the logarithm of the size, and high *clustering*. Other generalizations of the BA model with such properties have been defined in the literature (e.g., in [28, 29]).

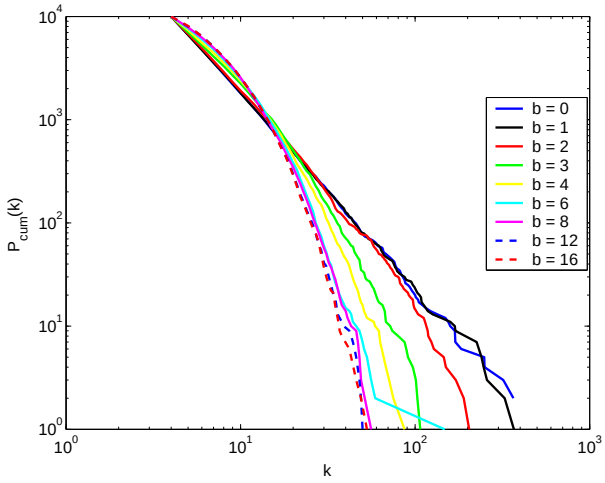

FIGURE 2. Cumulative degree distribution (in log-log scale) of the generalized Barabási-Albert model with $N = 10,000$ nodes and $< k >= 8$, for nine different values of the exponent b.

These models, however, do not take into account the physical distance between nodes, which in most real cases is an important parameter in the network evolution. For instance, in a neural network, it is more likely that a neuron connects to nearby neurons. Our model takes into account this phenomenon, weighting its importance with the exponent b. For $b > 2$, the GBA model also meets the requirements of low cost, which is fundamental for real-world networks.

2.3. **Brief comparison of topologies.** In this section, we briefly compare the models introduced above by means of the *characteristic path length*, the *clustering coefficient*, and the *structural cost* (see Table 1). For this static analysis, all the networks are built on a grid of $N = 10,000$ nodes and have an average degree $< k >= 8$. In accordance with [20], we have found that the regular lattice has high *clustering* (the 43% in comparison with the fully connected graph) and high *characteristic path length* (33.34); in contrast, the ER random graph has very low *clustering* (only the 0.06% in comparison with the fully connected graph) and low *characteristic path length* (4.66). It is worth noting that the ER model has a high cost (about 32 times greater than the cost of the lattice), because of the presence of many long-range connections.

The WS and NW small-world models (with probability p and q respectively equal to 0.08 and 0.0001) stay in between, preserving the high *clustering* of the lattice, at the expenses of a small increase of the *characteristic path length*, compared to the ER. Moreover, the cost of the WS and NW models is about six to nine times the cost of the lattice.

The values of the probabilities p for the WS model and q for the NW model have been set in order to have low characteristic path length, high clustering, and low cost.

As far as the BA and the GBA models are concerned, it is evident that, for increasing values of the exponent b, the *characteristic path length* increases very slowly. This is widely counterbalanced by the growth of the *clustering coefficient*

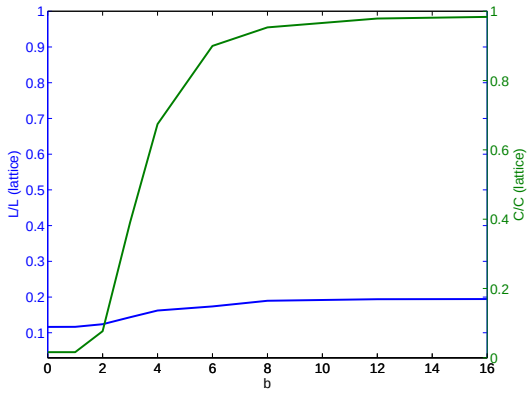

(a)

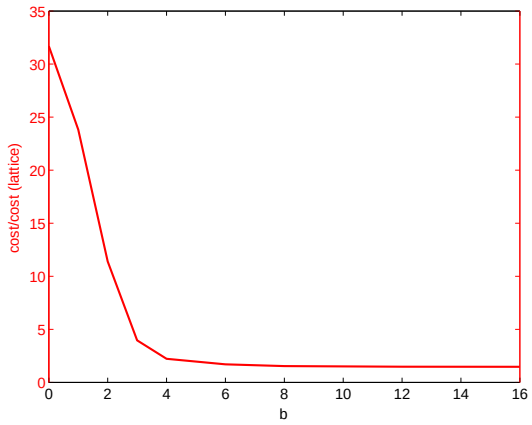

(b)

FIGURE 3. (a) *Characteristic path length* L (in blue) and *clustering coefficient* C (in green) for the GBA model with $N = 10,000$ nodes and average degree $< k >= 8$, as a function of the exponent b. (b) Structural cost as a function of the exponent b in the same condition as the top graph. Plotted quantities are divided by the corresponding quantity of the regular lattice with the same number of nodes and edges.

(which grows by a factor 24 from $b = 0$ to $b = 3$) and by the cutback of the cost (which is reduced by a factor 8 from $b = 0$ to $b = 3$).

In Table 1 the first models (lattice, ER, WS, and NW) are static, while the last ones (BA and GBA) are dynamic. The two networks that show a good compromise between L, C, and *cost* are the WS and the GBA. Particularly for the latter model, the optimal value of the exponent b is between 3 and 4. In the following, $b = 3$ will be used, because for this value the power-law degree distribution is better preserved. The WS has a *characteristic path length* and *clustering coefficient* higher than the GBA with $b = 3$. The GBA, however, being a dynamical model, is a more plausible representation of real-world networks.

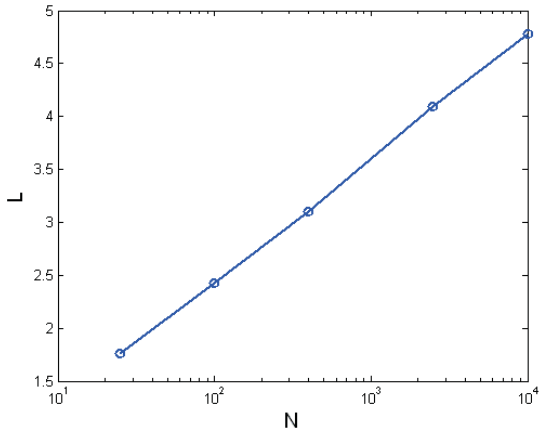

FIGURE 4. *Characteristic path length* for the GBA model with an exponent $b = 3$, as a function of the size of the network. The average degree is $< k >= 8$.

TABLE 1. A comparison between different topologies (see text for details).

	L	C	cost/cost (lattice)
Lattice	33.34	0.430	1.00
ER	4.66	0.0006	31.68
WS p=0.08	5.86	0.260	5.79
NW q=0.0001	5.08	0.286	8.77
BA	3.88	0.007	31.69
GBA b=3	4.78	0.168	3.96

3. **The neural model.** In the previous section, we have discussed the topological aspect for the representation of a neural network. In this section, we describe both neurons and synapses models, used in this paper.

3.1. **The Hindmarsh-Rose neuron.** In the literature, there are two different approaches to the problem of neuron modelling [30]:

- the former describes the ionic transportation processes in details;
- the latter aims at the characterization of the input-output relation for a certain number of physical measurable quantities.

In the first category, most models draw inspiration from the original Hodgkin-Huxley formalism [31], that describes a nonlinear dependence of the ionic permeability of the membrane from the membrane potential.

In the second category, the category of phenomenological models, the Hindmarsh-Rose neuron [32] is one of the most investigated. In the following, we will use this model, for which a single neuron is represented as a system of three ordinary differential equations:

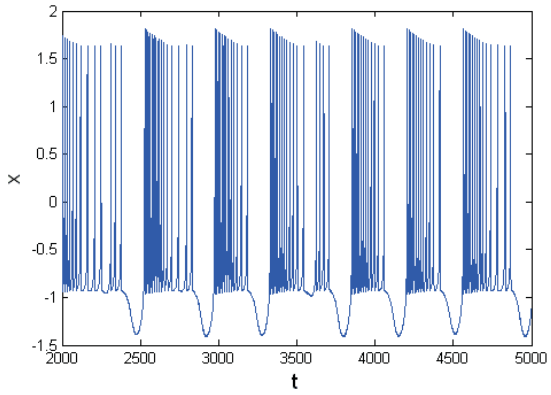

FIGURE 5. Time series for the membrane potential of Hindmarsh-Rose neuron (variable x).

$$\begin{cases} \frac{dx(t)}{dt} = y(t) + a \cdot x^2(t) - b \cdot x^3(t) - z(t) + I + I_{syn} \\ \frac{dy(t)}{dt} = c - d \cdot x^2(t) - y(t) \\ \frac{dz(t)}{dt} = r \cdot [s \cdot (x(t) + e) - z(t)], \end{cases} \tag{7}$$

where x is the membrane potential, and y and z represent respectively the fast and slow ionic channel dynamics. The parameters values have been chosen as in [10], to obtain a chaotic behavior ($a = 3$, $b = 1$, $I = 3.281$, $c = 1$, $d = 5$, $r = 0.0021$, $s = 4$, $e = 1.6$). An example of a time series for the membrane potential x is reported in Figure 5, which shows the typical bursting process.

Regarding the modelling of the synapse, it consists of two parts: the pre-synaptic terminal and the post-synaptic site, which may be located on the axon, soma, or dendrite of the nerve cell [18]. In the following sections, we will consider two different types of synapses: electrical and chemical. In both cases, the synaptic current I_{syn} is added to the right-side of the first differential equation of Equation (7).

3.2. **Electrical synapse.** The electrical synapse is based on the diffusion process, and is modelled as a resistance. For a particular node j, the synaptic current depends on the diffusion coefficient and on its own and its neighbors' membrane potential [10]:

$$I_{syn,j}(t) = D \cdot \sum_{i \in \mathbf{G}} a_{ij} \cdot (x_i(t) - x_j(t)), \tag{8}$$

where D is the diffusion coefficient.

In this kind of synapse, the delay is negligible and the electrical coupling results in the levelling of membrane potential. The electrical synapse is uncommon in the cortex of evolved animals.

3.3. **Chemical synapse.** The chemical synapse is the place where electrical signals coming from the axon of the presynaptic neuron are transduced in chemical

signals (in the synaptic cleft) and then again in electrical signals to travel in the dendrite of the postsynaptic neuron. Such a process can take place because of particular chemical intermediaries called neurotransmitters. When a presynaptic event occurs, a certain quantity of neurotransmitters is released in the synaptic cleft. The neurotransmitters spread quickly in the synaptic channel towards the postsynaptic site, where they form a chemical bond with the postsynaptic receptors. This gives rise to the increase of the conductance of the synapse, and hence to the presence of a post-synaptic current. The postsynaptic current I_{syn} is, therefore, directly proportional to the percentage of receptors bound with neurotransmitters [30]:

$$I_{syn,pre->post}(t) = g_{syn,pre->post}(t) \cdot [E_{syn} - x_{post}(t)] \tag{9}$$

$$g_{syn,pre->post}(t) = g_{synMax} \cdot r_{pre->post}(t) \tag{10}$$

$$r_{pre->post}(t) = \begin{cases} [r_{pre->post}(t_0) - r_\infty] \cdot e^{(t-t_0)/\tau_r} + r_\infty & if\ t_0 < t \leqslant t_0 + \tau \\ r_{pre->post}(t_0 + \tau) \cdot e^{-\beta \cdot (t - t_0 - \tau)} & if\ t > t_0 + \tau \end{cases} \tag{11}$$

$$r_\infty = \frac{\alpha \cdot T_{max}}{\alpha \cdot T_{max} + \beta} \tag{12}$$

$$\tau_r = \frac{1}{\alpha \cdot T_{max} + \beta}\ , \tag{13}$$

where $g_{syn}(t)$ is the actual conductance of the synapse at time t; g_{synMax} is the maximum conductance of the synapse (i.e. when all postsynaptic receptors are bound with neurotransmitters); $r(t)$ is the percentage of receptors bound with neurotransmitters (see Fig. 6); t_0 is the time at which the pre-synaptic event occurs, τ_r is a characteristic time constant; $T_{max} = 1$ is the maximum concentration of neurotransmitters at time t_0; α, β, and τ are parameters that we have fixed respectively as $\alpha = 2$, $\beta = 1$, and $\tau = 2$; and E_{syn} is the synaptic reversal potential (equal to 1.52 for an excitatory synapse and -1.36 for an inhibitory synapse), which is the value of the membrane potential for which no synaptic current flows in the ionic channel. Due to an electrical-chemical transduction, the chemical synapse introduces a delay, that is not constant for real neural networks [18]. The chemical synapse, unlike the electrical one, is directed, in the sense that a preferential direction exists in the information flux. Hence, if communication between nodes i and j can occur in both directions, it is because of the presence of two different uni-directional synapses, each with its parameters and its actual conductance.

4. **Dynamical analysis parameters.** In this section we present some parameters, that, together with the structural cost (Equation (4), will be useful for comparing the performance of each network.

4.1. **Synchronization index.** To evaluate the degree of synchronization of a system made of coupled units, we use the synchronization index σ [33]. Let matrix A collect in its rows all the N signals generated by the N subunits of the system and let $C^{(NxN)} = A \cdot A^T$ be the covariance matrix. The synchronization index takes into account the eigenvalues of C (the squares of the singular values of the matrix A). If all the signals are uncorrelated, all the singular values will be non-null. If

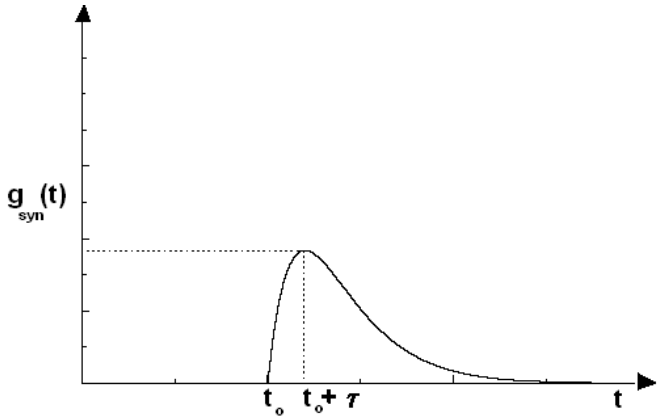

FIGURE 6. Percentage $r(t)$ of receptors bound with neurotransmitters as a function of time t. Time t_0 corresponds to the time of a pre-synaptic event.

all the signals are identical, we will find that only one singular value is different from 0; that is the rank of the matrix C is equal to 1. Of course if signals are similar but not identical, we will find very small but not null singular values. The synchronization index is thus defined at a certain percentage ξ, as the minimum number m of eigenvalues, whose sum is greater than a percentage of the trace of C:

$$\sigma(\xi) = min\ m\ \ | \sum_{i=1}^{m} \lambda_i^{sort} > \xi \cdot Tr(C), \tag{14}$$

where λ_i^{sort} is the i-th largest eigenvalue of the covariance matrix C.

If we have N neurons (and then N signals), this index varies in the range from 1 (when all signals are synchronized) to $[\xi N] + 1$ (when there is not synchronization) and gives information about the total number of different dynamics present in the system. In the following, we will consider the synchronization index to the 95%, because $N = 196$, $1 \leq \sigma(0.95) \leq 187$.

4.2. **Average power consumption.** Another important parameter here introduced is the average power consumption in information exchange.

In analogy with electrical systems, the average power consumption is defined in two ways, depending on the particular synapse model used. In the case of electrical synapses, we define the average power consumption $P_m(t_0, t_1)$ from time t_0 to time t_1 as:

$$P_m(t_0, t_1) = \sum_{i \neq j \in G} \frac{1}{t_1 - t_0} \cdot \int_{t_0}^{t_1} a_{ij} \cdot D \cdot \frac{1}{l_{ij}} \cdot [x_i(t) - x_j(t)]^2 dt \tag{15}$$

with

$$\frac{1}{R_{ij}} = a_{ij} \cdot D \cdot \frac{1}{l_{ij}}, \tag{16}$$

where R_{ij} represents the resistance between nodes i and j, a_{ij} is the element ij of the adjacency matrix, and l_{ij} is the physical distance between nodes i and j.

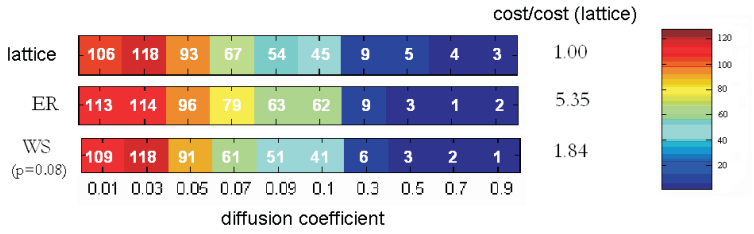

FIGURE 7. Synchronization index color maps as functions of the diffusion coefficient D for three networks with electrical synapses with different topology but fixed average degree $< k >= 4$. The structural cost (divided by the cost of the regular lattice) of the different networks is reported as well.

The average power consumption for the electrical synapses strictly depends on the differences of potentials $x_i - x_j$. For instance, if from time t_n the system is perfectly synchronized (i.e., $x_i(t) = x_j(t)$ for each i and j and for $t > t_n$), the average power consumption $P_m(t_n, +\infty)$ is null.

The average power consumption for the case of chemical synapses is instead defined as

$$P_m(t_0, t_1) = \sum_{i \neq j \in G} \frac{1}{t_1 - t_0} \cdot \int_{t_0}^{t_1} a_{ij} \cdot g_{syn,ij}(t) \cdot [E_{syn} - x_j(t)]^2 dt, \qquad (17)$$

where $g_{syn,ij}$ is the synaptic conductance between nodes i and j and E_{syn} is the synaptic potential. The average power consumption for chemical synapses, as defined here, considers only a localized dissipation, that does not takes into account the length of axons and dendrites.

5. **Dynamical effects of topology on synchronization.** The previous sections have focused on topologies and neural models as well as static and dynamical analysis parameters. This section addresses the topology effects on the synchronization of Hindmarsh-Rose neural networks.

The analysis has been carried out in two parts: the first describes the results obtained with electrical synapses and the second describes the results obtained with chemical synapses. In both cases, we have considered networks with $N = 196$ nodes.

5.1. **Neuron networks with electrical synapses.** First we compare the results of static topologies with the fixed average degree $< k >= 4$ as a function of the diffusion D. We have chosen the average degree $< k >= 4$, because we thus can distinguish more clearly the effects of different topologies. With greater values of $< k >$ in all the models, the number of edges increases, leading toward a fully connected network and thus hampering a clear differentiation of the effects of topologies.

In Figure 7, we report the synchronization index maps and the structural cost for various topologies (regular lattice, Erdös-Rényi random graph, Watts-Strogatz small-world model with $p = 0.08$). The maps are realized in 64 colors (from blue to red) in a scale of 128 values of the synchronization index (from 1 to 128), and thus

each color represents two values. As shown in section 4.1, the synchronization index ranges from 1 to 187, but we are not interested in distinguishing and representing values greater than 128, because they indicate the absence of synchronization. The results show that, for the region of low values of the diffusion coefficient (up to $D = 0.1$), none of the networks considered is able to synchronize. Therefore, in the following, we will neglect this region. For higher values of D, instead, the synchronization index σ becomes an interesting parameter for comparison.

The regular lattice, with its good local properties, reaches a minimum value $\sigma = 3$ for a diffusion coefficient $D = 0.9$. Although this means that the system has not reached a perfect synchronization, it shows a good synchronization for low-frequency behavior (bursts are simultaneous, spikes are asynchronous). This is evident in Figure 8, in which each subfigure is constituted by two parts. In the upper part, we report a color map for the N signals (corresponding to the N neurons of the network) as functions of time t. Colors range from blue to red for increasing values of the membrane potential x. In the lower part, we report three time series, corresponding to the output of three different neurons of the network.

The ER graph, with its good global properties, reaches very low values of the synchronization index σ. It means that in a network with electrical synapses, global properties weight more than local ones. Nevertheless, the ER graph costs more than five times the cost of the lattice.

The WS model produces an even better synchronization. It demonstrates that though global properties weight more than local ones, they are both fundamentally important for synchronization. Moreover, the WS model (for the chosen value of $p = 0.08$) has a structural cost much lower than the ER graph. The WS model is an optimal choice, for synchronization with the constraint of low-building cost.

To investigate how the choice of the rewiring probability p affects synchronization, structural cost, and power consumption, we have chosen a value of the diffusion coefficient ($D = 0.3$) leading to an imperfect synchronization dynamics. Figure 9 shows the three above mentioned quantities as functions of the probability of rewiring. The upper part of the figure shows that there is an intermediate wide range of the probability p for which the synchronization index is lower than the extreme cases of regular lattice ($p = 0$) and random graph ($p = 1$), confirming that both local and global connectivity help synchronization. As expected, because a greater rewiring introduces a greater number of long-range connections, the structural cost monotonically rises with p. Average power consumption follows almost the same trend of the synchronization index σ but depending on the square of the differences of membrane potentials, it is more sensitive to absolute differences of the potential.

An optimal choice for this model seems to be $p \simeq 0.08$, because of the low synchronization index, the low cost, and the modest average power consumption [34].

The analysis presented above is centered on a fixed value for the average degree ($< k >= 4$). Now we take into consideration the NW model, for which $< k >= 4$ is only the initial condition, and the average degree grows with the probability q of adding new edges. In Figure 10, we show the synchronization index σ color maps for different values of q. As expected, the system perfectly synchronizes when it is totally connected, because of the high coupling between all the neurons, at the expense of a very high cost (hundreds of times greater than the cost of the lattice). For the much smaller value of $q = 0.08$, we have found almost the same performance

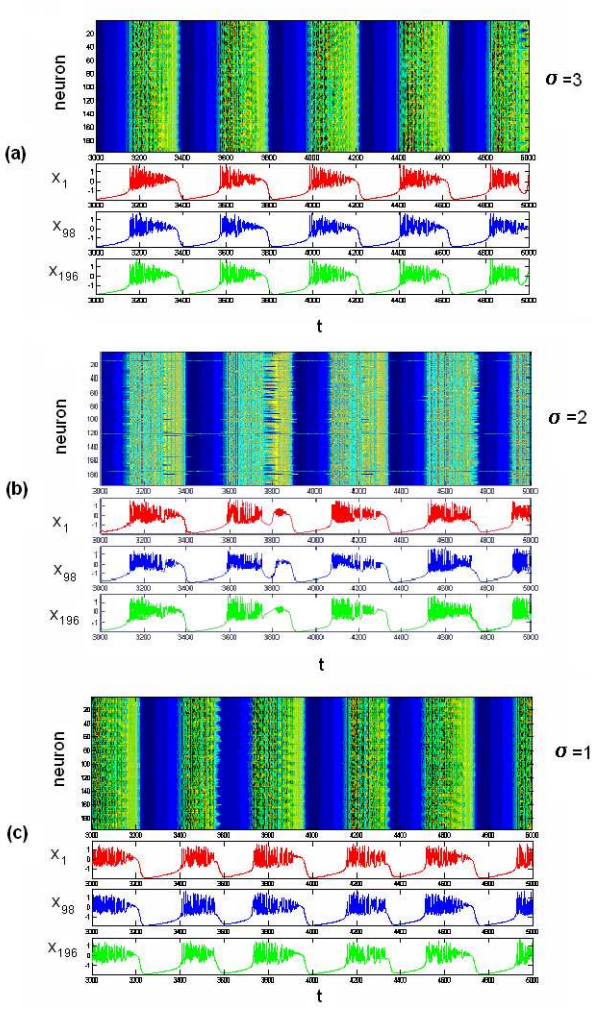

FIGURE 8. Space-time maps for three networks with electrical synapses. (a) Regular lattice; (b) Erdös-Rényi random graph; (c) Watts-Strogatz small-world model with a probability of rewiring $p = 0.08$.

as the totally connected network, but with a cost reduced by a factor of more than 100. Nevertheless, the cost is still too high. To obtain a cost comparable with the topologies investigated above, we have to reduce the probability q up to the value 0.01. For this value, we obtain an average degree $< k > \simeq 6$ and a cost that is almost four times the cost of the lattice with $< k >= 4$. In this case, for high values of the diffusion coefficient, we reach the perfect synchronization (see Fig. 11).

Furthermore, we have fixed a value of the diffusion coefficient ($D = 0.1$) and studied the synchronization index, the average power consumption, and the structural cost as functions of the probability q of adding edges (see Fig. 12). The results show that if the low structural cost is not a pressing requirement, the optimal value

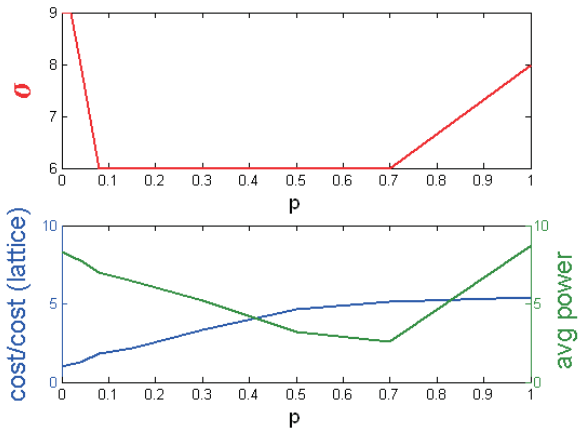

FIGURE 9. Synchronization index (in the upper part), structural cost and average power consumption (in the lower part) for the WS model as function of the probability of rewiring p. Limiting cases, that is, regular lattice ($p = 0$) and ER random graph ($p = 1$), are also considered.

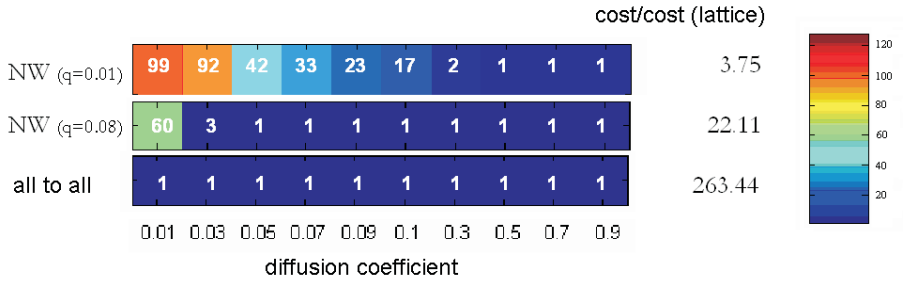

FIGURE 10. Synchronization index color maps as functions of the diffusion coefficient D for the NW model with electrical synapses for three different values of the probability q. The structural cost (divided by the cost of the regular lattice) of the different networks is reported as well.

of q is about 0.08, because of the perfect synchronization and the very low average power consumption.

The analysis presented above has shown the different behavior of static network models. Now we study the effects that the dynamical network models have on synchronization.

In Figure 13, we show the synchronization index color maps for the BA and the GBA with the exponent $b = 3$. It is evident that the slight decrease in synchronization for the GBA (see also Fig. 14) is counterbalanced by the structural cost, which is much lower than that of the BA model.

Comparing static and dynamical models, the WS model with $p = 0.08$, though having a cost lower than that of the GBA, has a higher average power consumption

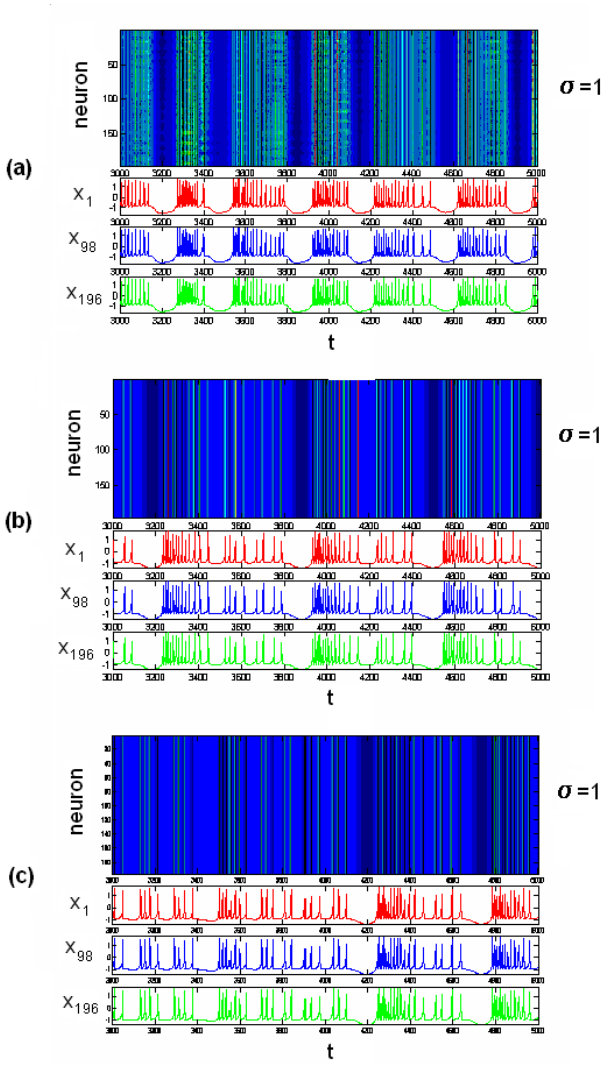

FIGURE 11. Space-time maps for the Newman-Watts model with $D = 0.9$ and with electrical synapses, for three different values of the probability q. (a) $q = 0.01$; (b) $q = 0.08$; (c) $q = 1.0$.

and the same degree of synchronization for high values of the diffusion coefficient (see Fig. 15).

We take into consideration an intermediate value of the diffusion coefficient ($D = 0.3$) and investigate the properties of the GBA model as functions of the parameter b (see Fig. 16). The synchronization index and the average power consumption increase with the exponent b. Nevertheless, this increase is widely counterbalanced by the remarkable reduction of the cost in the region around $b = 3$, which seems to be a suitable region.

5.2. **Neuron networks with chemical synapses.** In this section, neurons have been coupled by using chemical synapses as in Equations (9)–(13) with a value

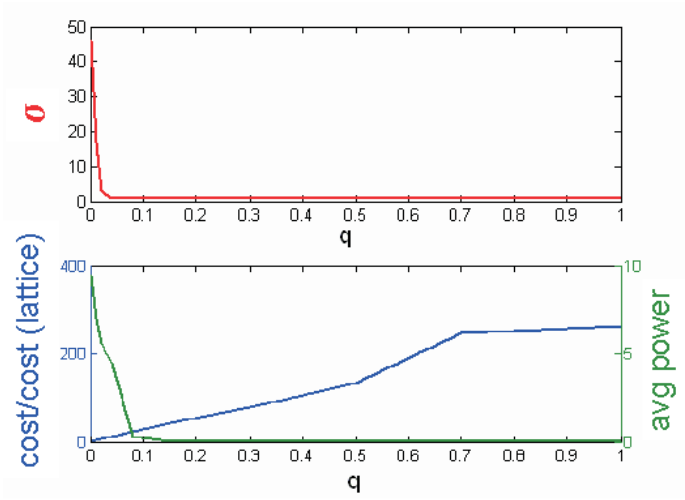

FIGURE 12. Synchronization index (in the upper part), structural cost and average power consumption (in the lower part) for the Newman-Watts small-world model with electrical synapses as function of the probability q of adding edges.

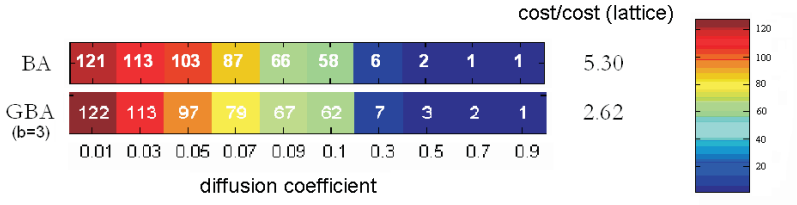

FIGURE 13. Synchronization index color maps as a function of the diffusion coefficient D for a BA (in the upper part) and a GBA network with $b = 3$ (in the lower part) with fixed average degree $< k >= 4$ and with electrical synapses. The structural cost (divided by the cost of the regular lattice) of the different networks is reported as well.

of $E_{syn} = 1.52$ (excitatory chemical synapses). In Figure 17, we show the synchronization index maps for five different topologies as functions of the maximum conductance g_{synMax}. The results are quite different from those obtained with the electrical synapse. The lattice is the topology that reaches the lowest values of the synchronization index. The ER random graph, on the contrary, cannot reach a value smaller than 16. Coherently, the WS model, being similar to the lattice but with some long-range connections (typical of the ER), shows values of the synchronization index σ that are slightly greater than those of the lattice. In Figure 18, the membrane potential of the $N = 196$ neurons is reported for the lattice, the ER graph, and the WS models.

The two types of synapses behave differently because the synchronization degree seems to play a different role in each type. In the electrical synapse, the diffusive

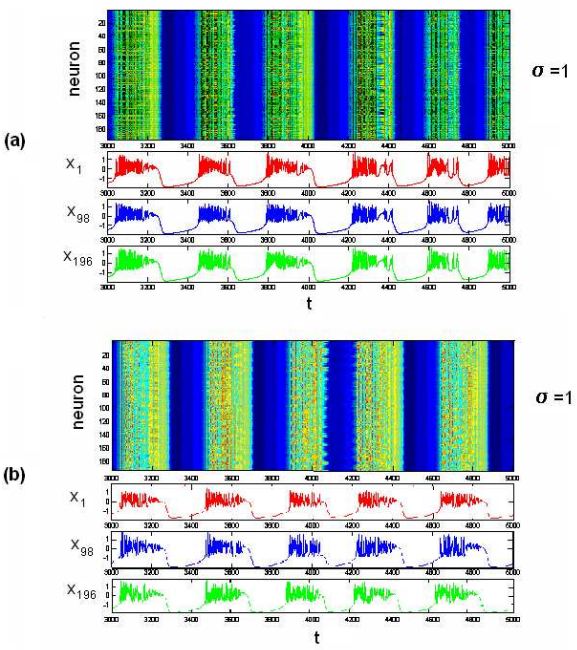

FIGURE 14. Space-time maps for two different networks with electrical synapses. (a) BA model and (b) GBA model for an exponent $b = 3$, both with $D = 0.9$.

effect tends to equalize the potential of connected neurons, independently of the number of neighbors. In the use of chemical synapses, the net input a neuron receives from synaptic neurons emitting synchronized spikes is proportional to the number of connected units (and thus to its degree). Hence, for chemical synapses, if all the nodes in a network have the same degree (as in the case of the lattice), synchronization will be enhanced; if different nodes have different degrees (as in the case of the ER random graph), synchronization will be hampered.

It is not surprising that the BA and the GBA models can reach values of the synchronization index lower than those of the ER. In fact, though these networks (having a wide range of variation in the degree of synchronization), are very heterogeneous, it should not be forgotten that many nodes have the same low degree [35]. It is the existence of these nodes that helps synchronization.

In Figure 19, the synchronization index and the average power consumption are plotted for all the analyzed networks. It is worth noting that the two topologies that show better synchronization (lattice and WS) have an optimal value of the maximum conductance $g_{synMax} = 0.8$, for which the synchronization index is minimal. In fact, further increasing the conductance not only produces an increase of the average power consumption, but also deteriorates the synchronization degree.

An analogous behavior is shown in Figure 20 for the same models, but with an average degree $< k >= 8$. The only difference is that the optimal value of the maximum conductance g_{synMax} for the lattice and the WS model is reduced to 0.4. As further confirmation, we compare, in Figure 21, the synchronization index and

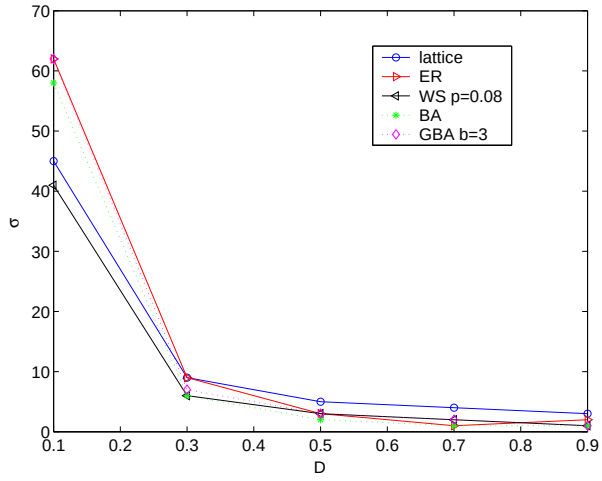

(a)

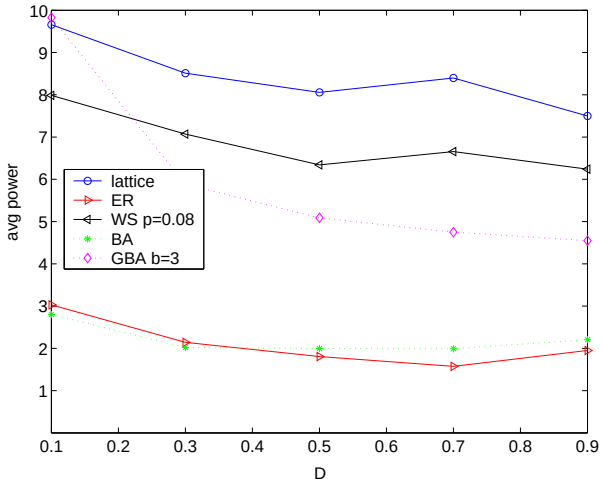

(b)

FIGURE 15. (a) synchronization index and (b) average power consumption for five different topologies with N=196 nodes, average degree $< k >= 4$, and electrical synapses as functions of the diffusion coefficient D.

the average power consumption for the lattice with average degrees $< k >= 4$ and $< k >= 8$.

6. **Conclusions.** In this paper we have analyzed the synchronization of Hindmarsh-Rose neural networks with two different types of synapse. We have studied such networks, placing the neurons on a two-dimensional grid with periodic boundary conditions, and connecting them according to the topologies of regular lattice, Erdös-Rényi random graph, Watts-Strogatz or Newman-Watts small-world models, and BA scale-free network. Moreover, we have developed a new model, based

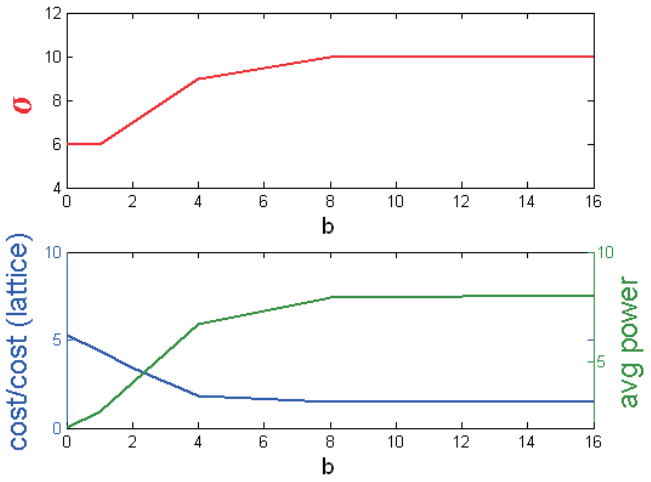

FIGURE 16. Synchronization index (in the upper part), structural cost and average power consumption (in the lower part) for the GBA model with electrical synapses as functions of b.

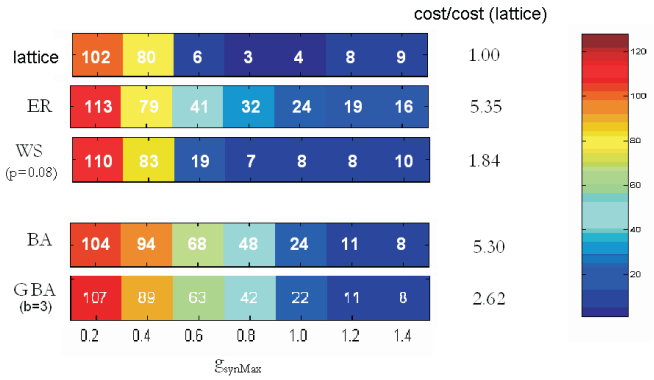

FIGURE 17. Synchronization index color maps as functions of the maximum conductance g_{synMax} for five networks with different topology but fixed average degree $< k >= 4$, with chemical synapses. From the top: regular lattice; Erdös-Rényi random graph; Watts-Strogatz small-world model with a probability of rewiring $p = 0.08$; BA model; and GBA model, with exponent $b = 3$.

on a generalization of the BA scale-free network that, taking into account that the edges formation is more likely between nodes with a short physical distance, seems more plausible for the characterization of a neural network. Such a model is characterized by a low *characteristic path length* as random graphs, and high clustering and a scale-free distribution and thus is particularly relevant since it conjugates both the features of a scale-free model and of a small-world network. For these

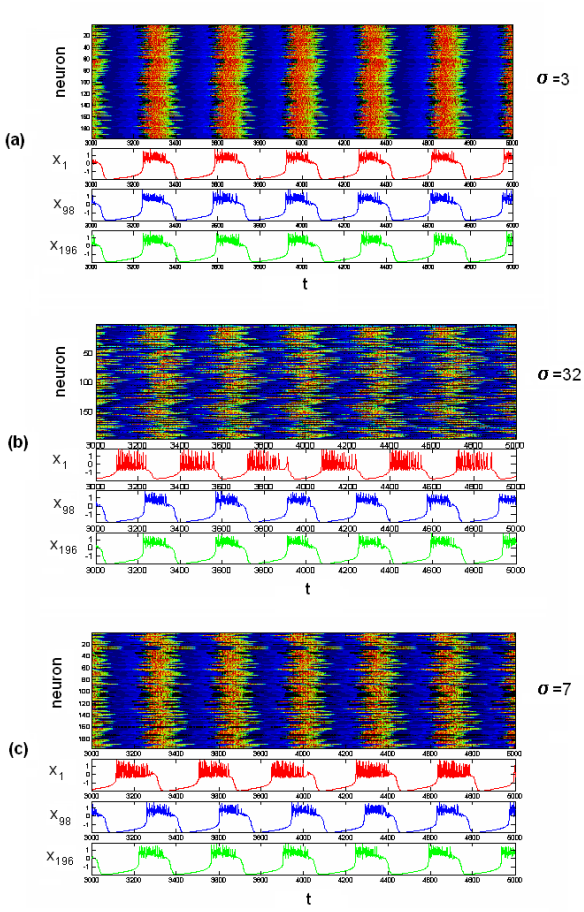

FIGURE 18. Space-time maps for three different networks with chemical synapses, with maximum conductance $g_{synMax} = 0.4$. From the top: regular lattice; Erdös-Rényi random graph, Watts-Strogatz small-world model with $p = 0.08$.

reasons, the new model can be applied to many other cases in which the dynamical evolution of the network is fundamental. Moreover, these characteristics have also been found to be very useful for the synchronization property of the network.

The analysis has been carried on by using numerical simulations. To further validate the results, the approach based on the so called master stability function [36], which has been successfully applied in many other cases [37, 11], can be used and will be addressed elsewhere. However, its application is restricted to the first part of the work. In fact, in the case of chemical synapses the coupling is neither linear nor static as required by the master stability function approach.

The results reported in this paper underline that in neuron networks synchronization depends strictly on the kind of synapse used in the networks. In the case of electrical synapses, the models that show a better trade-off between high synchronization and low structural and energetic costs are those with good global and local

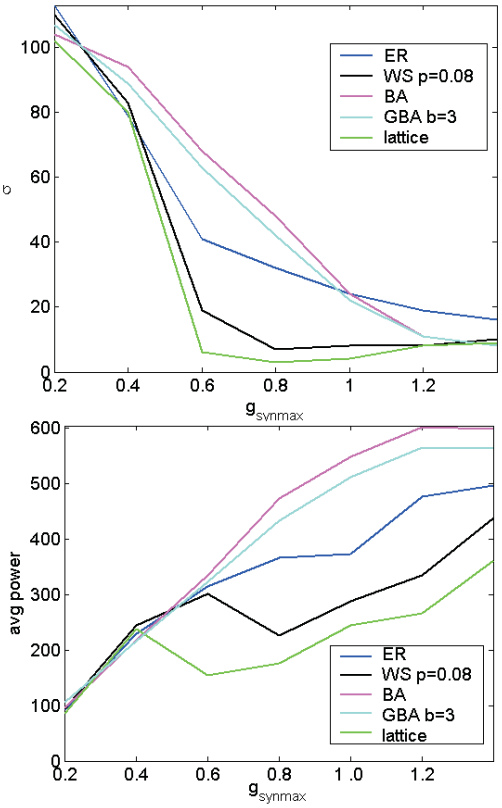

FIGURE 19. Synchronization index and average power consumption as functions of the maximum conductance g_{synMax} for: lattice, Erdös-Rényi random graph, Watts-Strogatz small-world with $p = 0.08$, BA and GBA models.

properties: among the static networks, the WS models and among the dynamical ones, the GBA models. On the contrary, in the case of chemical synapses, there is no real trade-off, because the lattice, thanks to its regularity, is the network with the best synchronization, lowest structural cost, and lowest average power consumption.

Moreover, we have developed a new methodology for the investigation of static and dynamical properties of neural networks, using some well-known parameters and introducing some new definitions. Such a methodology, used here to evaluate the effects of topology on Hindmarsh-Rose neural networks, is quite general and can be easily extended to in-depth studies of more realistic neural models, and to a possible design of artificial neural networks.

Acknowledgments. This work was supported partially by the Italian "Ministero dell'Istruzione, dell'Universit e della Ricerca" (MIUR) under the Firb project RBNE01CW3M.

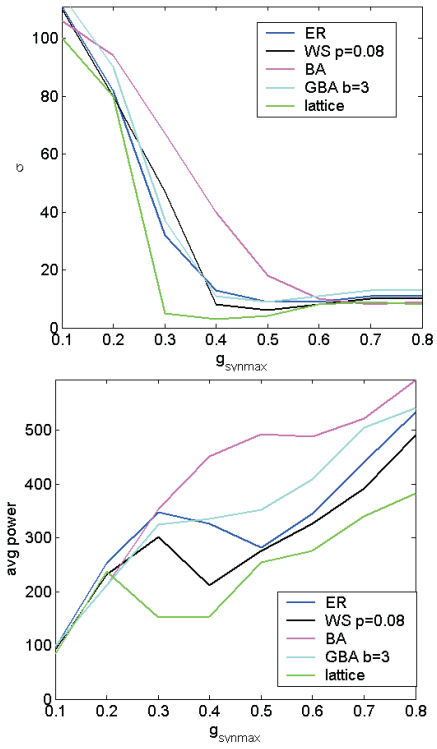

FIGURE 20. Synchronization index and average power consumption as functions of the maximum conductance g_{synMax} for lattice, Erdös-Rényi random graph, Watts-Strogatz small-world with $p = 0.08$, BA and GBA models in the case of $< k >= 8$ and chemical synapses.

REFERENCES

[1] X. F. Wang and G. Chen, SYNCHRONIZATION IN COMPLEX DYNAMICAL NETWORKS. Journal of Science and Complexity 16 (2003).

[2] Y. Braiman, J. F. Lidner and W. L. Ditto, TAMING SPATIOTEMPORAL CHAOS WITH DISORDER. Nature 378 (1995) 465–467.

[3] M. Gilli, INVESTIGATION OF CHAOS IN LARGE ARRAYS OF CHUA'S CIRCUITS VIA A SPECTRAL TECHNIQUE. IEEE Transactions on Circuits and Systems 42(10) (1995), 802–806.

[4] M. Bucolo, R. Caponetto, L. Fortuna, M. Frasca, and A. Rizzo, DOES CHAOS WORK BETTER THAN NOISE? IEEE Circuits and Systems Magazine 2 (3) (2002) 4–19.

[5] K. Y. Tsang, R. R. Mirollo, S. H. Strogatz and K. Wiesenfeld, DYNAMICS OF A GLOBALLY COUPLED OSCILLATOR ARRAY. Physica **D** 48 (1991) 102–112.

[6] Y. Braiman, W. L. Ditto, K. Wiesenfeld and M.L. Spano, DISORDER-ENHANCED SYNCHRONIZATION. Physics Letters **A** 206 (1995) 54–60.

[7] P. Arena, L. Fortuna, D.Porto, and A. Rizzo, SELF-ORGANIZATION IN ARRAYS OF NONLINEAR SYSTEMS INDUCED BY CHAOTIC PERTURBATION: AN EXPERIMENTAL APPROACH. ISCAS 99 Conference 5 (1999) 479–482.

[8] P. Arena, R. Caponetto, L. Fortuna, and A. Rizzo, NONORGANIZED DETERMINISTIC DISSYMMETRIES INDUCE REGULARITY IN SPATIOTEMPORAL DYNAMICS . Int. Journ. of Bifurc. and Chaos 10 (1) (2000) 73–85.

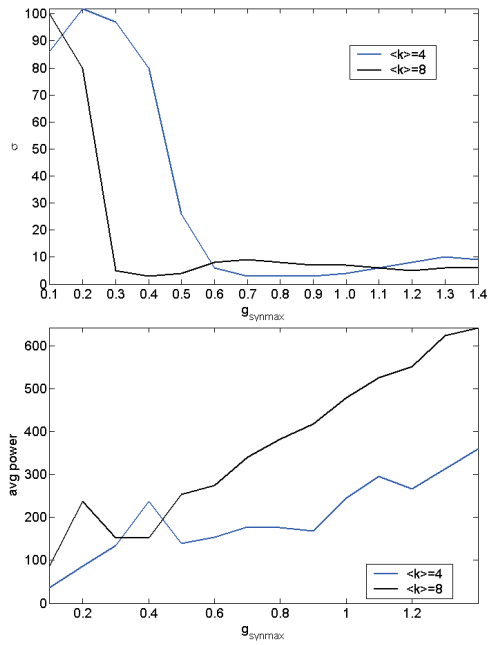

FIGURE 21. Synchronization index and average power consumption as functions of the maximum conductance g_{synMax} for the lattice with chemical synapses and with average degrees $< k >= 4$ and $< k >= 8$.

[9] P. Arena, R. Caponetto, L. Fortuna, M. La Rosa, and A. Rizzo, SELF-ORGANIZATION IN NONRECURRENT COMPLEX SYSTEMS. Int. Journ. of Bifurc. and Chaos 10, (2000).
[10] M. Bucolo, L. Fortuna, and M. La Rosa, NETWORK SELF-ORGANIZATION THROUGH SMALL-WORLDS TOPOLOGIES. Chaos, Solitons and Fractals 14 (2002) 1059–1064.
[11] M. Barahona and L. M. Pecora, SYNCHRONIZATION IN SMALL-WORLD SYSTEMS. Phys. Rev. **L** 89 (5) (2002) 054101.
[12] X. F. Wang and G. Chen, SYNCHRONIZATION IN SMALL-WORLD DYNAMICAL NETWORKS. Int. Journ. of Bifurc. and Chaos 12 (1) (2002) 187–92.
[13] X. F. Wang, COMPLEX NETWORKS TOPOLOGY, DYNAMICS AND SYNCHRONIZATION. Int. Journ. of Bifurc. and Chaos 12 (5) (2002) 885–916.
[14] S. H. Strogatz, EXPLORING COMPLEX NETWORKS. Nature 410 (2001) 268.
[15] S. Floyd and V. Jacobson, THE SYNCHRONIZATION OF PERIODIC ROUTING MESSAGES. IEEE/ACM Trans. Networking 2(2) (1994) 122–136.
[16] A. T. Winfree, THE GEOMETRY OF BIOLOGICAL TIME. Springer Verlag, New York, 1980.
[17] C. J. Peréz and K. Christensen, ON SELF-ORGANIZED CRITICALITY AND SYNCHRONIZATION IN LATTICE MODELS OF COUPLED DYNAMICAL SYSTEMS. Int. J. Mod. Phys. **B** 10 (1996) 1111–1151.
[18] H. D. I. Abarbanel, M. I. Rabinovich, A. Selverston, M. V. Bazhenov, R. Huerta, M. M. Sushchik and L. L. Rubchinskii, SYNCHRONISATION IN NEURAL NETWORKS. Physics–Uspekhi 39 (4) (1996) 337–362.
[19] M. Faloutsos, P. Faloutsos, C. Faloutsos, ON POWER-LAW RELATIONSHIPS OF THE INTERNET TOPOLOGY. Comput. Comm. Rev 29 (1999) 251.
[20] D. J. Watts and S. H. Strogatz, COLLECTIVE DYNAMICS OF SMALL-WORLD NETWORKS. Nature 393 (1998) 440–442.
[21] V. Latora and M. Marchiori, ECONOMIC SMALL-WORLD BEHAVIOR IN WEIGHTED NETWORKS. Europ. Phys. Journ. **B** 32 (2003) 249.
[22] P. Erdös and A. Rényi, ON RANDOM GRAPHS. Publicationes Mathematicae 6 (1959) 290.

[23] M. E. J. Newman and D. J. Watts, Renormalization group analysis of the small-world network model. Phys. Lett. **A** 263 (1999) 341–346.
[24] R. Albert, H. Jeong, and A.-L. Barabási, Internet: Diameter of the World-Wide Web. Nature 401 (1999) 130.
[25] A.-L. Barabási and R. Albert, Emergence of scaling in random networks. Science 286 (1999) 509.
[26] The initial edge configuration is not a key task for this model. Nevertheless, in order to avoid fractional values in the average node degree $< k >$, we have chosen to start with a fully connected network of $< k > +1$ nodes.
[27] Adding m edges per time step leads to a network with average degree $< k >= 2 \cdot m$.
[28] P. Holme and B. J. Kim, Growing Scale-Free Networks with Tunable Clustering. http://arxiv.org/abs/cond-mat/0402009 (2004).
[29] K. Klemm and V. M. Eguíluz, Growing scale-free networks with small-world behavior. Phys. Rev. **E** 65 (2002) 057102.
[30] M. Bove, M. Grattarola, G. Massobrio, M. Giugliano, and S. Martinoia. Dynamics of networks of biological neurons: simulation and experimental tool in Neural Network System Techniques and Applications, Algorithms and Architectures - vol. 1, Leondes, CT ed., Academic Press, San Diego, (1998), pp. 401–423.
[31] A. L. Hodgkin and A. F. Huxley, A quantitative description of membrane current and its application to conduction and excitation in nerve. J. Physiol. 117 (1952) 500–544.
[32] J. L. Hindmarsh and R. M. Rose, A model of neuronal bursting using three coupled first order differential equations. Proc. R. Soc. London Ser. **B** 221 (1984) 87–102.
[33] L. Fortuna, M. La Rosa, D. Nicolosi, and G. Sicurella, Spatio-temporal dynamics towards self-synchronization index. Proc. of the XII Int. IEEE Workshop on Nonlinear Dynamics of Electronic Systems, Évora, Portugal, 2004.
[34] It is not trivial to find a unique goodness parameter for the optimization of a network of dynamical systems. The choice cannot leave out of consideration the particular real application. If we are interested in building a large-scale device, our limiting parameter will be the cost, but if we are interested in building an autonomous system (e.g., a robot with on-board power supply), our attention will be mainly devoted to the power consumption.
[35] For instance, in the BA model with $N = 196$ nodes and average degree $< k >= 4$, there are 101 nodes (more than a half of the nodes of the network) with the same degree $k = 2$.
[36] L. M. Pecora and T. L. Carroll, Master Stability Functions for Synchronized Coupled Systems. Phys. Rev. Lett. 80(10) (1998) 2109–2112.
[37] T. Nishikawa, A. E. Motter, Y.-C. Lai, and F. C. Hoppensteadt, Heterogeneity in Oscillator Networks: Are Smaller Worlds Easier to Syncrhonize? Phys. Rev. Lett. 91(1) (2003) 014101.

Received on June 28, 2004. Revised on Aug. 2, 2004.

E-mail address: stefano.cosenza@tiscalinet.it
E-mail address: pacrucitti@ssc.unict.it
E-mail address: lfortuna@diees.unict.it
E-mail address: mfrasca@diees.unict.it
E-mail address: manuela.la-rosa@st.com
E-mail address: ceciliastagni@libero.it
E-mail address: lisausai@yahoo.it